

UCSF

UC San Francisco Previously Published Works

Title

Indigenous microbiota protects development of medication-related osteonecrosis induced by periapical disease in mice.

Permalink

<https://escholarship.org/uc/item/0837q6p3>

Journal

International journal of oral science, 14(1)

ISSN

1674-2818

Authors

Du, Wen

Yang, Mengyu

Kim, Terresa

et al.

Publication Date

2022-03-01

DOI

10.1038/s41368-022-00166-4

Copyright Information

This work is made available under the terms of a Creative Commons Attribution License, available at <https://creativecommons.org/licenses/by/4.0/>

Peer reviewed



ARTICLE OPEN

Indigenous microbiota protects development of medication-related osteonecrosis induced by periapical disease in mice

Wen Du^{1,2}, Mengyu Yang^{2,3}, Terresa Kim^{2,3}, Sol Kim^{2,3}, Drake W. Williams^{1,2,3}, Maryam Esmaeili^{2,3}, Christine Hong⁴, Ki-Hyuk Shin^{2,5}, Mo K. Kang^{2,5}, No-Hee Park^{2,5,6} and Reuben H. Kim^{2,3,5}✉

Bacterial infection is a common finding in patients, who develop medication-related osteonecrosis of the jaw (MRONJ) by the long-term and/or high-dose use of anti-resorptive agents such as bisphosphonate (BPs). However, pathological role of bacteria in MRONJ development at the early stage remains controversial. Here, we demonstrated that commensal microbiota protects against MRONJ development in the pulp-exposed periapical periodontitis mouse model. C57/BL6 female mice were treated with intragastric broad-spectrum antibiotics for 1 week. Zoledronic acid (ZOL) through intravenous injection and antibiotics in drinking water were administered for throughout the experiment. Pulp was exposed on the left maxillary first molar, then the mice were left for 5 weeks after which bilateral maxillary first molar was extracted and mice were left for additional 3 weeks to heal. All mice were harvested, and cecum, maxilla, and femurs were collected. ONJ development was assessed using μ CT and histologic analyses. When antibiotic was treated in mice, these mice had no weight changes, but developed significantly enlarged ceca compared to the control group (CTL mice). Periapical bone resorption prior to the tooth extraction was similarly prevented when treated with antibiotics, which was confirmed by decreased osteoclasts and inflammation. ZOL treatment with pulp exposure significantly increased bone necrosis as determined by empty lacunae and necrotic bone amount. Furthermore, antibiotics treatment could further exacerbate bone necrosis, with increased osteoclast number. Our findings suggest that the commensal microbiome may play protective role, rather than pathological role, in the early stages of MRONJ development.

International Journal of Oral Science (2022)14:16

; <https://doi.org/10.1038/s41368-022-00166-4>

INTRODUCTION

Anti-resorptive treatment (ART) with agents such as bisphosphonate (BPs) or denosumab (Dmab) is commonly practiced in patients with osteoporosis and bone metastatic diseases.¹ In patients undergoing a long-term ART, a rare intraoral lesion called medication-related osteonecrosis of the jaw (MRONJ) may develop, which is clinically defined as exposed bone through intraoral and/or extraoral fistula that persists for more than 8 weeks without a history of radiation therapy.^{2,3}

Several risk factors are known to be associated with MRONJ development such as duration and/or administration route of medication,^{4,5} dentoalveolar surgery,^{6–8} and local inflammatory lesion.^{9,10} Among them, dentoalveolar trauma is one of the major risk factors for development of MRONJ. It has been reported that a tooth extraction or dental surgery is the precipitating event that causes ONJ in 78% of the cases.² Studies also showed that extraction can increase the risk of having ONJ by 33 folds.^{3,6} Given that most tooth extractions are operated to resolve pre-existing pathological lesions including periodontal or periapical diseases,^{3,11,12} it has been suggested that the pre-existing local inflammatory lesions initiated by bacterial infection may already have predisposed the affected area to developing MRONJ following tooth extraction.^{13–17}

Bacterial infection and host's inflammation play an important role in development of periodontal and periapical diseases.^{18,19}

Studies have shown that pathogenic bacteria colonize tooth extraction sites in animals and humans with bisphosphonate treatment, exacerbating ONJ development.^{20–22} In line with this observation, cancer patients exhibit a decrease in ONJ incidence upon improved oral hygiene, which indicates an important role of bacterial infections in MRONJ.²³ Microbial biofilm formation on sequestered bone has been revealed by using scanning electron microscope analysis,²⁴ and fluorescence in situ hybridization using the probe targeting 16S rDNA showed the presence of increased bacterial staining in ONJ lesions in an animal model.²⁵ Collectively, these studies suggest that the presence of bacteria is associated with MRONJ; however, its etiological role in initiating MRONJ development is still elusive.

We recently attempted to address this question by using a mouse model that combines ligature-induced periodontitis and extraction-induced MRONJ under a condition that significantly suppressed bacterial loads with wide spectrum antibiotics (ABX). Surprisingly, ABX treatment further exacerbates the extraction-induced MRONJ with the pre-existing periodontitis, suggesting that indigenous microbiota protects from developing ONJ.²⁵

¹State Key Laboratory of Oral Diseases & National Clinical Research Center for Oral Diseases & Department of Prosthodontics, West China Hospital of Stomatology, Sichuan University, Chengdu, China; ²The Shapiro Family Laboratory of Viral Oncology and Aging Research, Los Angeles, USA; ³Section of Restorative Dentistry, UCLA School of Dentistry, Los Angeles, USA; ⁴Department of Orofacial Sciences, UCSF School of Dentistry, San Francisco, USA; ⁵UCLA Jonsson Comprehensive Cancer Center, Los Angeles, USA and ⁶David Geffen School of Medicine at UCLA, Los Angeles, USA

Correspondence: Reuben H. Kim (rkim@dentistry.ucla.edu)

Received: 2 December 2021 Accepted: 21 February 2022

Published online: 21 March 2022

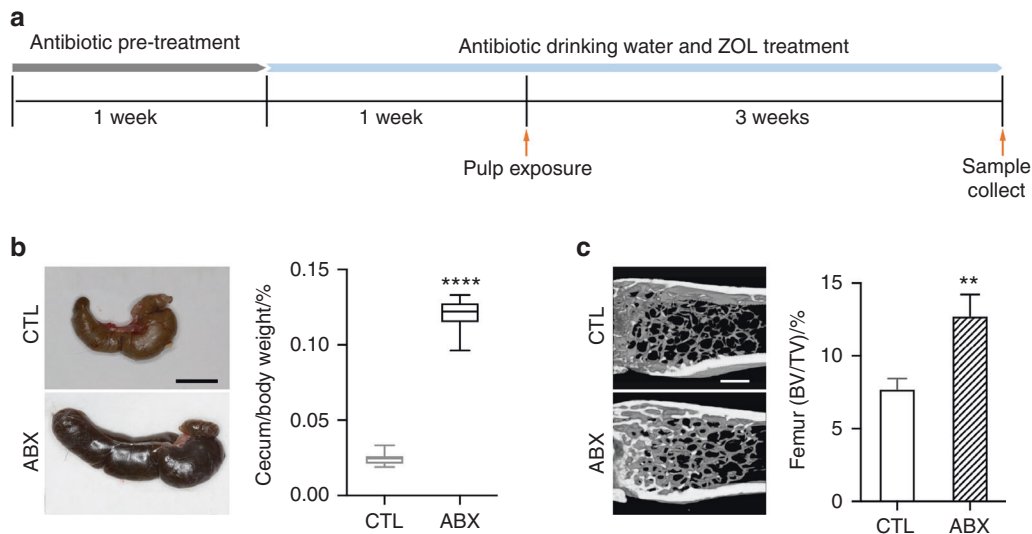


Fig. 1 Broad-spectrum antibiotic treatment alters cecal weight and bone volume. **a** Schematic of pulp exposure mouse model with broad-spectrum antibiotic treatment. For a detailed description, please refer to section of “Materials and methods” **b** Representative images of ceca from control (CTL) and antibiotic treated (ABX) mice and the percentage of cecum weight to total animal body weight at the time of sacrifice. **c** Representative images of the metaphyseal trabecular bone from the distal femur and quantification of bone volume (BV/TV). All quantified data represent mean \pm SEM ($n = 8$). $^{**}P < 0.01$; $^{****}P < 0.0001$. The scale bars represent 10 mm in **b** and 500 μ m in **c**

Unlike the periodontal disease, periapical diseases result from the penetration of bacteria through the infected pulp, with subsequent inflammation and bone resorption at the root apex of affected tooth. Therefore, we deleted bacterial loads using broad spectrum ABX and assessed bone mass, osteonecrosis development, osteoclast, and immune cell number, trying to investigate whether indigenous bacteria function as an etiological factor in initiating MRONJ using our previously established mouse model that combines pulp-exposed periapical periodontitis and tooth extraction-induced MRONJ.^{26,27}

RESULTS

Broad-spectrum antibiotic treatment prevented pulp exposure-induced periapical radiolucency in mice

We first aim to examine the effect of reduced commensal microbiota on apical periodontitis after pulp exposure. To do so, a mixture of intragastric and intraoral gavage of antibiotics (ABX) or PBS were administered for 1 week. Then, antibiotics were administered in the drinking water for additional week, after which the pulp was exposed. Mice were left for 3 weeks after pulp exposure until sacrifice (Fig. 1a). Consistent with the previous findings,²⁵ ABX-treated mice exhibited enlarged ceca (Fig. 1b) and increased bone volume (Fig. 1c), both of which are important physiologic phenotypes associated with antibiotic-treated mice due to depleted oral and GI microbiome.²⁸ When bone resorption around the root apices were examined, ABX-treated mice exhibited less bone loss compared to the saline-treated mice (Fig. 2a, b), suggesting that broad-spectrum antibiotic treatment reduced commensal microbiota and prevented bone resorption at the root apices mediated by pulp exposure.

Broad-spectrum antibiotic treatment reduced numbers of osteoclasts and inflammatory cells at the apices of pulp-exposed tooth in mice

To further examine the effect of reduced commensal microbiota on apical periodontitis after pulp exposure at the cellular level, we assessed the presence of osteoclasts and inflammatory cells. Histological examination revealed intense infiltration of inflammatory cells at the apex of saline-treated mice. With ABX treatment, the inflammation at the apex was diminished (Fig. 2c). Similarly, the

numbers of TRAP + osteoclasts were decreased (Fig. 3a). In line with these observations, we detected less numbers of CD66b⁺ granulocytes and CD3⁺ T-cells (Fig. 3b, c). These data indicate that ABX prevented pulp exposure-induced bone resorption and periapical radiolucency by reducing the numbers of osteoclasts and inflammatory cells.

Reduced commensal microbiota exacerbates osteonecrosis induced by periapical inflammation

To determine the role of the commensal microbiota in the onset of ONJ development, we implemented our previously established MRONJ mouse model. The left side of the maxillary first molar was exposed to induce periapical periodontitis and after 5 weeks the extraction were then performed on the same tooth as well as the contralateral first molar. Then after 3 weeks of healing, the samples are harvested (Fig. 4a). Consistent with our previous study, μ CT images showed that unfilled sockets were present in pulp-exposed tooth-extracted sites of zoledronic acid (ZOL)-treated group,²⁷ and they were more prominent in ABX-treated group (Fig. 4b). To determine whether the bony sequelae in the tooth-extracted socket is associated with pulp-exposure induced ONJ under ABX treatment, we quantify the newly formed bone in tooth extracted socket. ZOL treatment can overall reduces new bone formation, indicating the inductive role of ZOL in tooth extraction-induced ONJ development through inhibiting or delaying the healing process. With pulp exposure, ABX treatment further inhibited new bone formation compared with control mice in ZOL-treated group (Fig. 4c), which suggests that the depletion of microbiota might cause more severe damage to the alveolar bone with the ONJ development.

Osteonecrosis was then evaluated the by the number of empty lacunae and amount of necrotic bone through histological approach. The result showed that with the extraction, the presence of BPs induced empty lacunae and necrotic bone, and pulp exposure could further induce osteonecrosis in ZOL-treatment group (Fig. 5a–c, $P < 0.05$). Interestingly, ABX treatment exacerbated osteonecrosis demonstrated by significantly increased necrotic bone and empty lacunae in pulp-exposed site with ZOL administration (Fig. 5a–c, $P < 0.05$). Further analysis showed that more TRAP + osteoclasts were exhibited in ZOL-treated mice regardless of pulp exposure (Fig. 6a, b, $P < 0.05$).

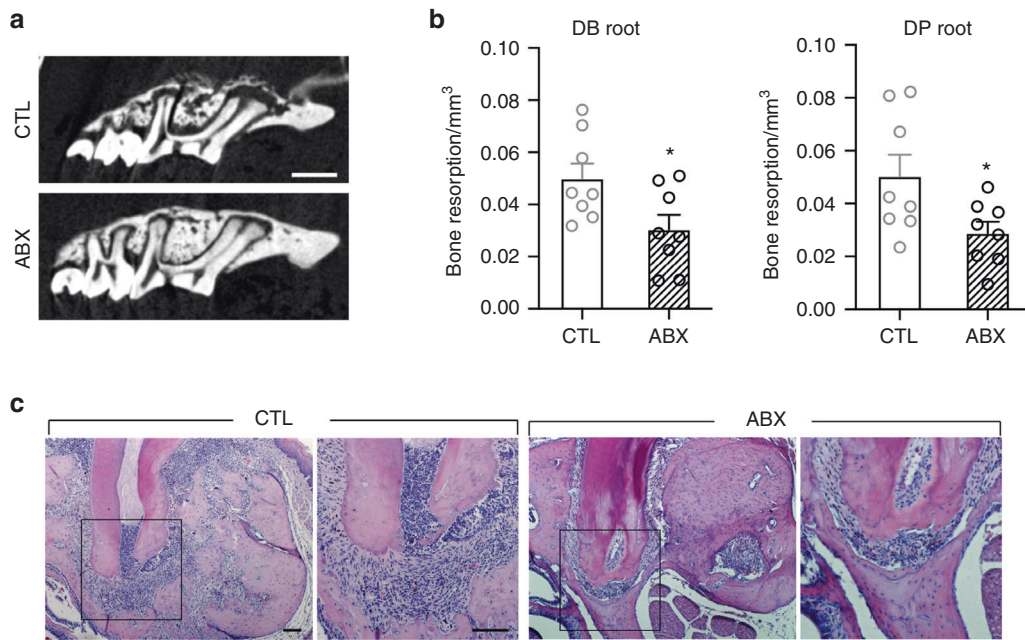


Fig. 2 Antibiotic treatment prevents the development of periapical radiolucency (PARL) and inflammation at the apex. **a** μ CT scans of pulp exposed tooth from CTL and ABX mice. **b** Quantification of total bone resorption in the apex of distobuccal (DB) and distopalatal (DP) roots on the exposed first maxillary molar. **c** Representative images of H&E staining at the apex of pulp exposed tooth. All quantified data represent mean \pm SEM ($n = 8$). * $P < 0.05$. The scale bars represent 500 μ m in **a** and 100 μ m in **c**

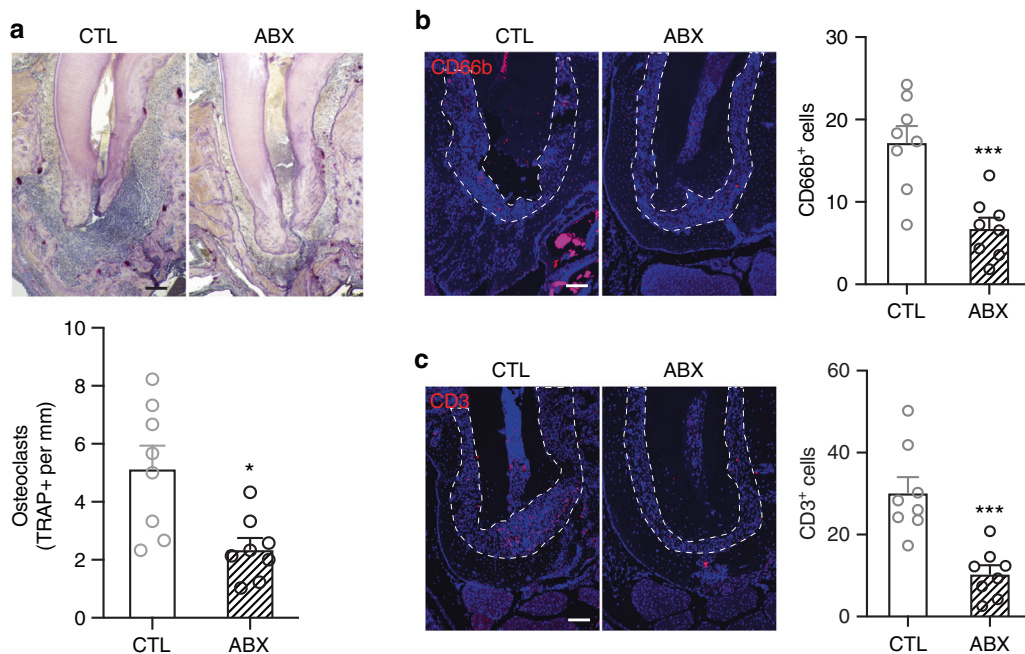


Fig. 3 Antibiotic treatment reduces the number of osteoclasts and immune cells at the apex area of pulp exposed tooth. **a** Representative images and quantification of TRAP + osteoclast number at the apex of pulp exposed tooth. **b**, **c** Representative images and quantification of immunofluorescent staining for CD66b⁺ (**b**) and CD3⁺ (**c**) cells at the apex area of pulp exposed tooth. Dashed lines outline the area where CD66b⁺ and CD3⁺ cells were counted. All quantified data represent mean \pm SEM ($n = 8$). * $P < 0.05$; *** $P < 0.001$. Scale bar: 100 μ m

Within the ZOL-treated group, ABX administration could induce the number of TRAP + osteoclasts, which is more obvious in the pulp-exposed site (Fig. 6a, b, $P < 0.05$). When we examined CD66b⁺ and CD3⁺ cells, we found no difference in their numbers regardless of antibiotic treatment (Fig. 6c, d), suggesting persistent ongoing inflammatory responses. Taken together, our results indicate that with BPs and pre-existing periapical disease, ABX treatment induces osteonecrosis formation and osteoclasts

number, but does not significantly affect the number of CD66b⁺ granulocytes and CD3⁺ T-cells (Fig. 6e).

DISCUSSIONS

Bacterial infection is a common finding in MRONJ patients and the degree of infection is associated with MRONJ advancement.^{23,29} Indeed, the use of antibiotics has been suggested as a standard of

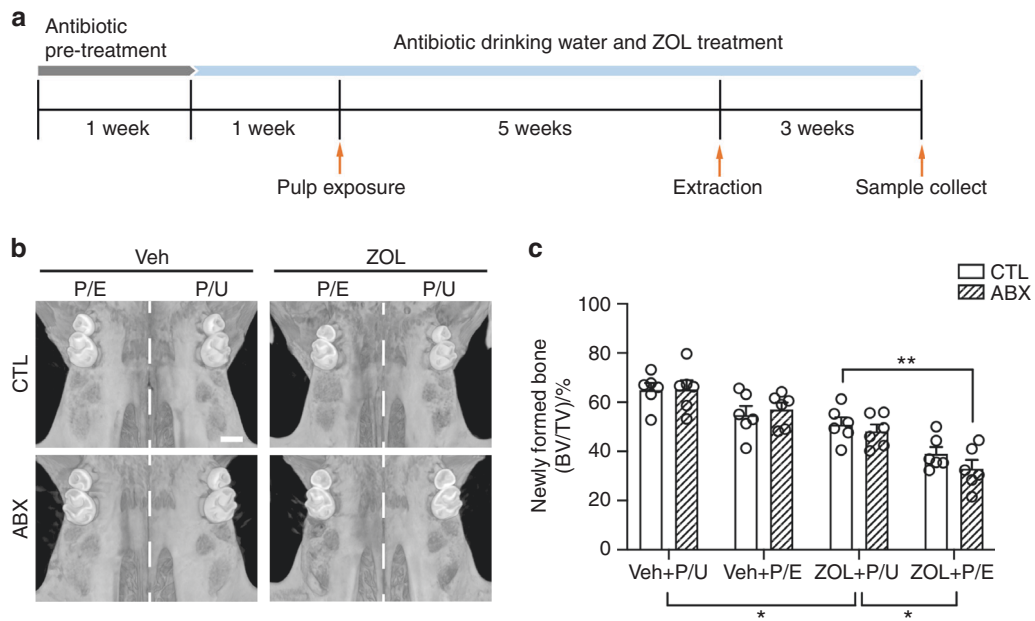


Fig. 4 Establishment of pulp exposure and tooth extraction MRONJ mice model with broad-spectrum antibiotic treatment. **a** Schematic diagram of the experiment. For a detailed description, please refer to section of “Materials and methods”. **b** The uCT scans of the maxillae after the sample were harvested. **c** Quantification of newly formed bone in tooth extracted socket (BV/TV). P/E pulp exposed, P/U pulp unexposed. All quantified data represent mean \pm SEM ($n = 6$). * $P < 0.05$; ** $P < 0.01$. Scale bar: 500 μm

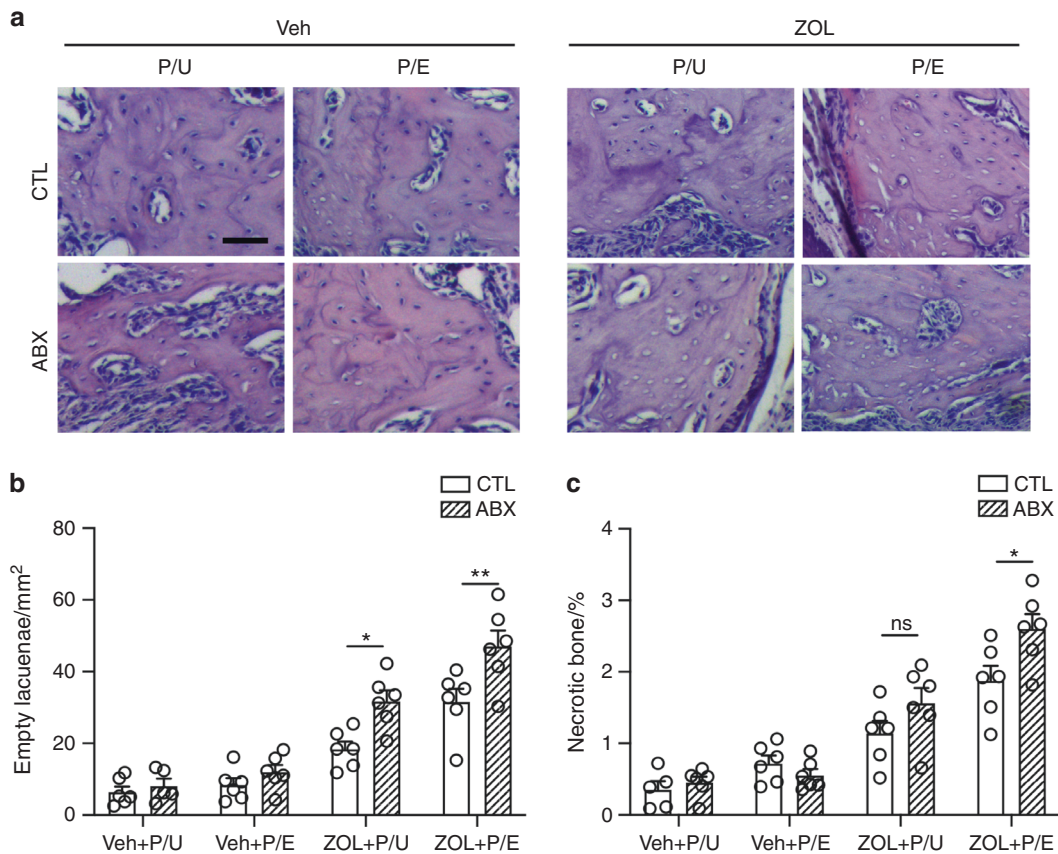


Fig. 5 Reduction of commensal microbiota exacerbates periapical periodontitis-mediated MRONJ development. **a** Representative images of H&E staining at the site of extraction. **b** Quantification of empty lacunae number. **c** Quantification of necrotic bone presented as a percentage of the total bone area. P/E pulp exposed, P/U pulp unexposed. All quantified data represent mean \pm SEM ($n = 5-6$). * $P < 0.05$; ** $P < 0.01$; ns, not statistical significant. Scale bar: 50 μm

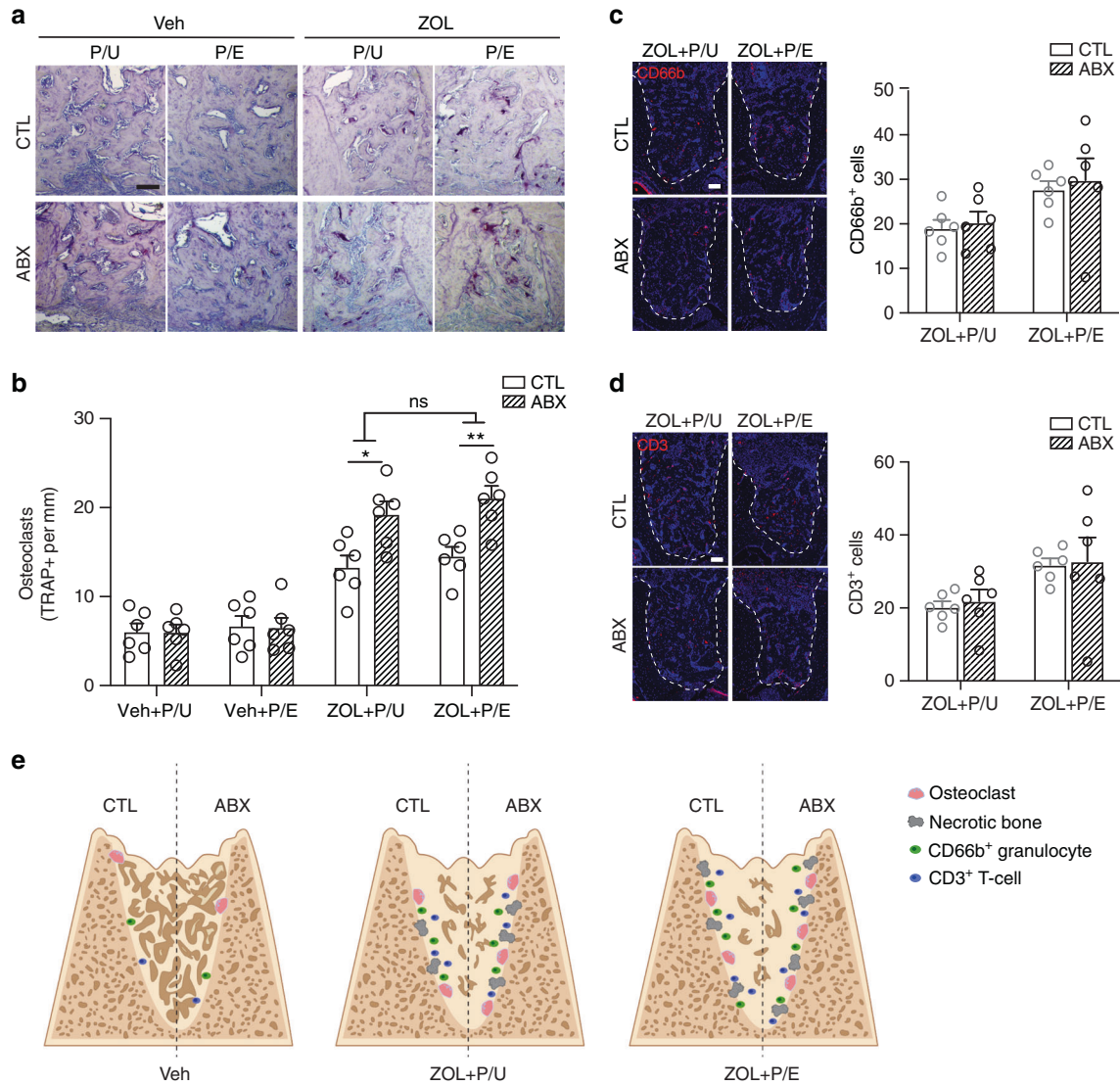


Fig. 6 Assessment of osteoclasts and immune cells in dysbiotic mice. **a** TRAP staining with aniline blue counterstain at the tooth extracted site. **b** Quantification of TRAP + osteoclast number per bone surface. **c, d** Representative images and quantification of immunofluorescent staining for CD66b⁺ (**c**) and CD3⁺ (**d**) cells at the tooth extracted site in BP treated mice. Dashed lines outline the area where CD66b⁺ and CD3⁺ cells were counted. **e** Proposed model with tooth extraction. Antibiotic (ABX) does not alter the number of osteoclasts or necrotic bone formation in Veh mice (left). Under zoledronic acid (ZOL) treatment (center and right), ABX treatment leads to increased necrotic bone and osteoclast number. ABX does not alter the number of CD66b⁺ and CD3⁺ immune cells regardless of pulp exposure. P/E pulp exposed, P/U pulp unexposed. All quantified data represent mean ± SEM (n = 6). *P < 0.05; **P < 0.01; ns, not statistical significant. Scale bar: 100 μm

care in patients with ongoing MRONJ.³ However, the etiological role of bacterial infection that may cause MRONJ development in the beginning stage is not clearly defined.

Depletion of indigenous commensal oral and GI microbiota using antibiotic treatment is routinely used to examine the role of commensal microbiota.³⁰ Previously, we used the similar method to reduce the indigenous microbiota in mice that are pre-disposed to inflammatory condition (e.g., ligature-induced periodontitis) and subsequent tooth extraction in the presence of bisphosphonate.²⁵ LIP is a well-established model to mimic periodontitis in mice because ligature entraps bacteria and accumulation of dental plaque.^{31,32} However, the ligature placement also causes the physical trauma, complicating interpretation whether inflammation is truly induced by bacteria or consistent physical trauma by ligature itself. In this study, we predisposed the mice to another inflammatory condition (e.g., pulp exposure) and examine the direct effects of reduced commensal microbiota in ONJ development. The current study demonstrated that commensal microbiota

did not contribute to the etiological role of initiating MRONJ development; rather, significant reduction of commensal microbiota exacerbated development of MRONJ (Fig. 5a–c), suggesting that indigenous microbiota may have protective role in ONJ development and that a delicate balance between reducing pathogenic bacteria and preserving the indigenous oral flora is an important factor in ONJ development.

Previously, it was shown that BPs disturbed the healing process by inhibiting woven bone formation in the tooth-extracted sockets.^{27,33} Consistent with this observation, the current model also caused diminished new bone formation in the tooth-extracted sites (Fig. 4b, c). BPs inhibit appositional new bone formation by impairing osteoclasts' resorptive function and osteoclast–osteoblast coupling.^{33,34} Interestingly, germ-free condition in mice is associated with increased bone mass and diminished osteoclast differentiation.³⁵ Given that BPs are known to increase the numbers of non-attached osteoclasts,³⁶ and that both BPs and ABX impair osteoclasts' functions, it explains

increased bone necrosis (Fig. 5a–c) and decreased new bone formation in the tooth-extracted sockets (Fig. 4b, c) when there are more osteoclasts present in ZOL and ABX group (Fig. 6a, b).

We previously demonstrated that the use of ABX in mice significantly altered oral microbiota composition in mice by directly measuring 16S rDNA gene copies from bacteria in the ligature as well as examining cecum size and bone volume.²⁵ In this study, we were not able to demonstrate directly the composition of the oral microbiota due to technical difficulties in collecting samples from the root canal or periapical lesions. However, enlarged ceca were similarly exhibited in mice with antibiotics (ABX) treatment for four weeks at which the size of the cecum the ABX-treated mice became an average of four times more than that from the CTL mice (Fig. 1b). In addition, ABX treatment significantly increased the bone volume as indicated by the BV/TV ratio (Fig. 1c), indicating that ABX regimen in this study has functionally altered oral microbiota composition in the root canals.

It is noteworthy that, although ABX treatment alone reduced inflammation at the root apex after pulp exposure (Fig. 3b, c), ABX treatment in the presence of ZOL failed to reduce inflammation (Fig. 6c, d). Indeed, while both CD66b⁺ granulocytes and CD3⁺ T-cells, the predominant cells in the innate and the adaptive immune system,³⁷ respectively, were decreased by ABX treatment alone, no inflammation was reduced even with ABX treatment in the presence of ZOL. It was previously showed that bisphosphonate-treated osteoclasts triggered increased release of pro-inflammatory mediators such as IL6, TNF- α , and IL-1 β .³⁸ In our study, ZOL treatment increased the numbers of osteoclasts (Fig. 6a, b), which is in line with the previous report that dysregulated osteoclasts are known to be associated with long-term bisphosphonate users.³⁹ Because bounded form of BPs is highly inert whereas free form of BPs asserts biological activities, it is tempting to speculate that short life span of matured osteoclasts due to free form of BPs while resorbing the bone surface induces increases in osteoclasts formation and homing as a feedback mechanism. As such, it is probable that continual ZOL treatment over long period of time may have caused increased inflammatory condition by recruited osteoclasts that released pro-inflammatory factors.

On the other hand, other agents such as denosumab or bevacizumab that are known to cause ONJ do not induce, if not reduce, inflammation.^{40,41} Although the direct effects of denosumab or bevacizumab on inflammation in the context of MRONJ development warrant further examination, induction of inflammatory signals by the drug itself may not fully explain the persistent inflammation even with the ABX treatment.

Alternatively, persistent inflammation during the ABX treatment may be associated with impaction of debris in the root canals from the oral environment such as food, which was frequently observed in our model (Fig. 2c and 3a). Pulp exposure in germ-free condition also induced small degree of inflammation due to impacted food or debris.⁴² Furthermore, occlusal trauma is also known to elicit pulpal inflammation and exacerbate periapical lesion.⁴³ These non-bacteria associated factors may explain persistent pulpal inflammation and continual destruction of the local environment to cause ONJ development in combination with BP.

A previous study showed that the use of antibiotic prophylaxis that starts before 3 days and lasts until 4 days after tooth extraction significantly lowered MRONJ development in rats.¹⁷ In line with this, ectopic introduction of *Fusobacterium nucleatum* after tooth extraction caused development of MRONJ-like lesions in mice.⁴⁴ As such, prophylactic antibiotic treatment has been recommended in the clinic when a tooth extraction is indicated in patients who are taking anti-resorptive agents. On the other hand, in our study, we significantly reduced the bacterial loads throughout study and found that long-term antibiotic treatment

may exacerbate MRONJ development. Based on these notions, it implies that while short-term antibiotic regimen may help reducing the incidence of developing ONJ lesions, a long-term excessive treatment with antibiotics may contribute significantly to ONJ development. Knowing this fine balance of using antibiotic regimens in ONJ patients would be imperative to mitigate this detrimental lesion in the oral cavity.

MATERIALS AND METHODS

Animals

Six-week-old C57BL/6J female mice were purchased from the Jackson Laboratories (Stock no. 000664) and kept in a specific pathogen free environment in the UCLA Division of Laboratory and Animal Medicine (DLAM). All experimental protocols were approved by institutional guidelines from the Chancellor's Animal Research Committee (2011–062).

The mouse model of periapical lesion

Mice were intraperitoneally injected with ketamine/xylazine (100 and 5 mg kg⁻¹ body weight, respectively) for anesthesia. The pulp of left maxillary first molar was exposed by a high-speed 1/4 round bur on a portable dental unit (Aseptico Inc., Woodinville, WA). The pulp exposure was performed under endodontic microscope (BM-LED stereo microscope, MEIJI Techno, Japan) with $\times 10$ magnification. Exposed tooth was left open without any coverage. As a control, contralateral maxillary first molar was not pulp-exposed during the study.

Commensal microbiota reduction and osteonecrosis development Mice were assigned into four groups randomly: control (CTL)/Veh, antibiotic-treated (ABX)/Veh, CTL/Zoledronic acid (ZOL), and ABX/ZOL ($n = 8–10$ mice each). During the first 7 days of the study, a mixture of intragastric and intraoral gavage of neomycin (100 mg·kg⁻¹), vancomycin (50 mg·kg⁻¹) and metronidazole (100 mg·kg⁻¹) were administered to mice in ABX/Veh and ABX/ZOL group twice daily while ampicillin (0.5 mg·mL⁻¹) dissolved in the drinking water ad libitum. At the same time, the mice in CTL/Veh and CTL/ZOL received sterile saline gavage and unaltered drinking water. After the first 7 days, ABX mice were provided with a mixture of neomycin (1 mg·mL⁻¹), vancomycin (0.5 mg·mL⁻¹), and ampicillin (1 mg·mL⁻¹) in drinking water ad libitum, while 0.9% NaCl or 125 μ g·kg⁻¹ Zoledronic acid (Sagent Pharmaceuticals) were respectively administered in the Veh and ZOL groups through intravenous injections biweekly for the remainder of the study. One week after the end of gavage administration, pulp of the left maxillary first molar was exposed in all mice to induce periapical periodontitis. The mice that were used to examine periapical periodontitis development were sacrificed 3 weeks after pulp exposure (Fig. 1a). To induce MRONJ in the remaining mice, the exposed tooth as well as the contralateral healthy tooth were extracted after 5 weeks of pulp exposure. After three additional weeks healing, the animals were euthanized by CO₂ followed by cervical dislocation. Maxilla, femur, and ceca of each mouse were harvested for further analysis. A schematic illustration indicating the timeline of the study is provided in Fig. 3a.

Micro-computed tomography (μ CT)

The mouse maxillae and femur were scanned with a voxel size of 10 μ m³ through a 1.0 mm aluminum filter at 60 kVp and 166 μ A (SkyScan 1275; Bruker). Two-dimensional reconstruction images were generated by N Recon (Bruker) with X-Y alignment and dynamic range adjustment. Three-dimensional representative images were generated in CTvox (Bruker). Morphological parameters of trabecular bone microarchitecture in femur were evaluated by CTAn (Bruker microCT, Kontich, Belgium).⁴⁵ Epiphyseal growth plate was defined to be the starting point of region of interest (ROI) and three-tenths of total femur length was

calculated as the size of ROI. Bone volume fraction (BV/TV; %) of the femur from each mouse was collected by measure bone volume (BV; mm³) and the total volume (TV; mm³). Newly formed bone in the tooth-extracted sites, displayed as percentage of BV/TV, was also quantified by selecting a volume containing the distal lingual, distal buccal, and mesial roots.

Tissue preparation

The maxillae were harvested and fixed in 4% paraformaldehyde in PBS (pH 7.4) overnight at 4 °C. Then 70% ethanol was used to store these fixed maxillae, which were subjected to μ CT scanning. After scanning, the tissue was transferred into daily-changed decalcification solution of 5% EDTA and 4% sucrose in PBS, pH 7.4 at 4 °C for 2–3 weeks, and decalcification solution was changed daily. Decalcified tissues were subsequently sent to UCLA Translational Procurement Core Laboratory (TPCL) for processing and paraffin embedding. The embedded tissue were sectioned at the coronal plane in a series of 5 μ m thickness.

Tartrate-resistant acid phosphatase (TRAP) histochemical staining TRAP staining were performed following the protocol described previously.³³ Four slides per sample were deparaffinized at 60 °C, then rehydrated in ethanol with an increasing concentration of water. The rehydrated tissue slides were stained with TRAP solution (#387A-1KT, Millipore Sigma) for 30 min in dark, then washed with water and counterstained with hematoxylin for 8 s. The number of osteoclasts which were identified with the presence of multiple nuclei ($n > 5$) was counted using ImageJ software after the pictures were taken by microscope (model DP72; Olympus) at $\times 100$ magnification.

Histomorphometric analysis

Empty lacunae number and necrotic bone areas were measured according to previously described protocol.³³ H&E staining was performed to the sectioned slides ($n = 4$, every five cuts) from each sample. After the tissue were rehydrated, the sectioned slides were stained with hematoxylin for 2.5 min, and then washed with water and 95% ethanol before stained with eosin for 1 min. The stained slides were then dehydrated in 70%, 95%, and 100% ethanol followed by xylene. Slides were mounted using mounting medium (Permount; Fisher Scientific, Houston, TX) and digital images were taken by microscope (model DP72; Olympus) at $\times 100$ magnification. The total bone surface area was measured using ImageJ software, and the number of empty lacunae per total bone area (#/mm²) were calculated. Necrotic bone was determined as a bone area that has at least five empty lacunae per 1 mm², and the total necrotic bone areas will be divided by total bone area to get the percentage of necrotic bone.

Immunofluorescence staining

Paraffin embedded tissues were rehydrated, and antigen retrieval was performed in citrate buffer at 60 °C overnight. Sections were blocked in 10% normal goat serum and incubated in primary antibody against CD3 (1:200, #ab5690, Abcam) and CD66b (1:200, #ab197678, Abcam) diluted in 3% serum overnight. After washes in PBST for three times, incubation with secondary antibody diluted in 3% serum was performed for 1 h followed by counterstaining with DAPI for 8 min. Slides were mounted using Prolong Gold (P36930; ThermoFisher Scientific) and images were taking using a confocal microscope (LSM700; Zeiss). CD3⁺ and CD66b⁺ cells were counted in the area (outlined by dashed lines in Figs. 3b, c and 6c, d) around the root apex after pulp exposure or within the tooth extracted socket after tooth extraction.

Statistical analysis

Single factor ANOVA and Tukey's post hoc test were performed to compare the μ CT data of trabecular bone measurements (BV/TV), empty lacunae number, necrotic bone (%), and number of

osteoclast among different groups. All statistical analyses were performed through Prism 8 software.

DATA AVAILABILITY

All data used/analyzed in this article are contained within the manuscript or available from the corresponding authors upon reasonable request.

ACKNOWLEDGEMENTS

This study was supported National Institutes of Health/National Institute of Dental and Craniofacial Research (grant DE023348 to R.H.K.; grant DE025172 to D.W.W.) and China Postdoctoral Science Foundation (grant 2019M663526 to W.D.).

AUTHOR CONTRIBUTIONS

W.D. contributed to conception, design, data acquisition, analysis, and interpretation, drafted and critically revised the manuscript; M. Y., T.K., S.K., D.W.W., and M.E., contributed to data acquisition and analysis, critically revised the manuscript; C.H., K.H.S., M.K.K., N.H.P., contributed to data interpretation, critically revised the manuscript; R.H.K. contributed to conception, design, data interpretation, drafted, and critically revised the manuscript. All authors gave final approval and agree to be accountable for all aspects of the work.

ADDITIONAL INFORMATION

Competing interests: The authors declare no competing interests.

REFERENCES

- Chen, J. S. & Sambrook, P. N. Antiresorptive therapies for osteoporosis: a clinical overview. *Nat. Rev. Endocrinol.* **8**, 81–91 (2011).
- Marx, R. E., Sawatari, Y., Fortin, M. & Broumand, V. Bisphosphonate-induced exposed bone (osteonecrosis/osteopetrosis) of the jaws: risk factors, recognition, prevention, and treatment. *J. Oral Maxillofac. Surg.* **63**, 1567–1575 (2005).
- Ruggiero, S. L. et al. American Association of Oral and Maxillofacial Surgeons position paper on medication-related osteonecrosis of the jaw-2014 update. *J. Oral Maxillofac. Surg.* **72**, 1938–1956 (2014).
- Henry, D. H. et al. Randomized, double-blind study of denosumab versus zoledronic acid in the treatment of bone metastases in patients with advanced cancer (excluding breast and prostate cancer) or multiple myeloma. *J. Clin. Oncol.* **29**, 1125–1132 (2011).
- Martins, A. S. et al. Relevant factors for treatment outcome and time to healing in medication-related osteonecrosis of the jaws—a retrospective cohort study. *J. Craniomaxillofac. Surg.* **45**, 1736–1742 (2017).
- Vahtsevanos, K. et al. Longitudinal cohort study of risk factors in cancer patients of bisphosphonate-related osteonecrosis of the jaw. *J. Clin. Oncol.* **27**, 5356–5362 (2009).
- Soundia, A. et al. Zoledronate impairs socket healing after extraction of teeth with experimental periodontitis. *J. Dent. Res.* **97**, 312–320 (2018).
- Saad, F. et al. Incidence, risk factors, and outcomes of osteonecrosis of the jaw: integrated analysis from three blinded active-controlled phase III trials in cancer patients with bone metastases. *Ann. Oncol.* **23**, 1341–1347 (2012).
- Yamazaki, T. et al. Increased incidence of osteonecrosis of the jaw after tooth extraction in patients treated with bisphosphonates: a cohort study. *Int. J. Oral Maxillofac. Surg.* **41**, 1397–1403 (2012).
- Aghaloo, T. L. et al. Periodontal disease and bisphosphonates induce osteonecrosis of the jaws in the rat. *J. Bone Miner. Res.* **26**, 1871–1882 (2011).
- Ficarra, G. et al. Osteonecrosis of the jaws in periodontal patients with a history of bisphosphonates treatment. *J. Clin. Periodontol.* **32**, 1123–1128 (2005).
- Boonyapakorn, T., Schirmer, I., Reichart, P. A., Sturm, I. & Massenkeil, G. Bisphosphonate-induced osteonecrosis of the jaws: prospective study of 80 patients with multiple myeloma and other malignancies. *Oral Oncol.* **44**, 857–869 (2008).
- Kim, T. et al. Removal of pre-existing periodontal inflammatory condition before tooth extraction ameliorates medication-related osteonecrosis of the jaw-like lesion in mice. *Am. J. Pathol.* **188**, 2318–2327 (2018).
- Mawardi, H. et al. Sinus tracts—an early sign of bisphosphonate-associated osteonecrosis of the jaws? *J. Oral Maxillofac. Surg.* **67**, 593–601 (2009).
- Kang, B. et al. Periapical disease and bisphosphonates induce osteonecrosis of the jaws in mice. *J. Bone Miner. Res.* **28**, 1631–1640 (2013).
- Aguirre, J. I. et al. Oncologic doses of zoledronic acid induce osteonecrosis of the jaw-like lesions in rice rats (*Oryzomys palustris*) with periodontitis. *J. Bone Miner. Res.* **27**, 2130–2143 (2012).

17. Lopez-Jornet, P. et al. Perioperative antibiotic regimen in rats treated with pamidronate plus dexamethasone and subjected to dental extraction: a study of the changes in the jaws. *J. Oral Maxillofac. Surg.* **69**, 2488–2493 (2011).
18. Nair, P. N. On the causes of persistent apical periodontitis: a review. *Int. Endod. J.* **39**, 249–281 (2006).
19. Stashenko, P., Teles, R. & D'Souza, R. Periapical inflammatory responses and their modulation. *Crit. Rev. Oral Biol. Med.* **9**, 498–521 (1998).
20. Katsarelis, H., Shah, N. P., Dhariwal, D. K. & Pazianas, M. Infection and medication-related osteonecrosis of the jaw. *J. Dent. Res.* **94**, 534–539 (2015).
21. Kos, M. et al. Pamidronate enhances bacterial adhesion to bone hydroxyapatite. Another puzzle in the pathology of bisphosphonate-related osteonecrosis of the jaw? *J. Oral Maxillofac. Surg.* **71**, 1010–1016 (2013).
22. Sedghizadeh, P. P. et al. Microbial biofilms in osteomyelitis of the jaw and osteonecrosis of the jaw secondary to bisphosphonate therapy. *J. Am. Dent. Assoc.* **140**, 1259–1265 (2009).
23. Ripamonti, C. I. et al. Decreased occurrence of osteonecrosis of the jaw after implementation of dental preventive measures in solid tumour patients with bone metastases treated with bisphosphonates. The experience of the National Cancer Institute of Milan. *Ann. Oncol.* **20**, 137–145 (2009).
24. Sedghizadeh, P. P. et al. Identification of microbial biofilms in osteonecrosis of the jaws secondary to bisphosphonate therapy. *J. Oral Maxillofac. Surg.* **66**, 767–775 (2008).
25. Williams, D. W. et al. Indigenous microbiota protects against inflammation-induced osteonecrosis. *J. Dent. Res.* **99**, 676–684 (2020).
26. Song, M. et al. Development of a direct pulp-capping model for the evaluation of pulpal wound healing and reparative dentin formation in mice. *J. Vis. Exp.* (2017).
27. Song, M. et al. Preexisting periapical inflammatory condition exacerbates tooth extraction-induced bisphosphonate-related osteonecrosis of the jaw lesions in mice. *J. Endod.* **42**, 1641–1646 (2016).
28. Gordon, H. A. & Pesti, L. The gnotobiotic animal as a tool in the study of host microbial relationships. *Bacteriol. Rev.* **35**, 390–429 (1971).
29. Dimopoulos, M. A. et al. Reduction of osteonecrosis of the jaw (ONJ) after implementation of preventive measures in patients with multiple myeloma treated with zoledronic acid. *Ann. Oncol.* **20**, 117–120 (2009).
30. Reikvam, D. H. et al. Depletion of murine intestinal microbiota: effects on gut mucosa and epithelial gene expression. *PLoS ONE* **6**, e17996 (2011).
31. Graves, D. T., Kang, J., Andriankaja, O., Wada, K. & Rossa, C. Jr Animal models to study host-bacteria interactions involved in periodontitis. *Front. Oral Biol.* **15**, 117–132 (2012).
32. Abe, T. & Hajishengallis, G. Optimization of the ligature-induced periodontitis model in mice. *J. Immunol. Methods* **394**, 49–54 (2013).
33. Williams, D. W. et al. Impaired bone resorption and woven bone formation are associated with development of osteonecrosis of the jaw-like lesions by bisphosphonate and anti-receptor activator of NF-kappaB ligand antibody in mice. *Am. J. Pathol.* **184**, 3084–3093 (2014).
34. Kozutsumi, R. et al. Zoledronic acid deteriorates soft and hard tissue healing of murine tooth extraction sockets in a dose-dependent manner. *Calcif. Tissue Int.* **110**, 104–116 (2022).
35. Sjogren, K. et al. The gut microbiota regulates bone mass in mice. *J. Bone Miner. Res.* **27**, 1357–1367 (2012).
36. Kuroshima, S., Go, V. A. & Yamashita, J. Increased numbers of nonattached osteoclasts after long-term zoledronic acid therapy in mice. *Endocrinology* **153**, 17–28 (2012).
37. Lakschevitz, F. S. et al. Identification of neutrophil surface marker changes in health and inflammation using high-throughput screening flow cytometry. *Exp. Cell Res.* **342**, 200–209 (2016).
38. Tseng, H. C. et al. Bisphosphonate-induced differential modulation of immune cell function in gingiva and bone marrow in vivo: role in osteoclast-mediated NK cell activation. *Oncotarget* **6**, 20002–20025 (2015).
39. Weinstein, R. S., Roberson, P. K. & Manolagas, S. C. Giant osteoclast formation and long-term oral bisphosphonate therapy. *N. Engl. J. Med.* **360**, 53–62 (2009).
40. Ferrari-Lacraz, S. & Ferrari, S. Do RANKL inhibitors (denosumab) affect inflammation and immunity? *Osteoporos. Int.* **22**, 435–446 (2011).
41. Merida, S. et al. Bevacizumab diminishes inflammation in an acute endotoxin-induced Uveitis model. *Front. Pharm.* **9**, 649 (2018).
42. Kakehashi, S., Stanley, H. R. & Fitzgerald, R. J. The effects of surgical exposures of dental pulps in germ-free and conventional laboratory rats. *Oral Surg. Oral Med. Oral Pathol.* **20**, 340–349 (1965).
43. Matsumoto, T. et al. Factors affecting successful prognosis of root canal treatment. *J. Endod.* **13**, 239–242 (1987).
44. Mawardi, H. et al. A role of oral bacteria in bisphosphonate-induced osteonecrosis of the jaw. *J. Dent. Res.* **90**, 1339–1345 (2011).
45. Bouxsein, M. L. et al. Guidelines for assessment of bone microstructure in rodents using micro-computed tomography. *J. Bone Miner. Res.* **25**, 1468–1486 (2010).



Open Access This article is licensed under a Creative Commons Attribution 4.0 International License, which permits use, sharing, adaptation, distribution and reproduction in any medium or format, as long as you give appropriate credit to the original author(s) and the source, provide a link to the Creative Commons license, and indicate if changes were made. The images or other third party material in this article are included in the article's Creative Commons license, unless indicated otherwise in a credit line to the material. If material is not included in the article's Creative Commons license and your intended use is not permitted by statutory regulation or exceeds the permitted use, you will need to obtain permission directly from the copyright holder. To view a copy of this license, visit <http://creativecommons.org/licenses/by/4.0/>.

© The Author(s) 2022